

pubs.acs.org/JPCL Letter

Electric Fields Influence Intramolecular Vibrational Energy Relaxation and Line Widths

Anwesha Maitra, Sohini Sarkar, David M. Leitner, and Jahan M. Dawlaty*



Cite This: J. Phys. Chem. Lett. 2021, 12, 7818-7825



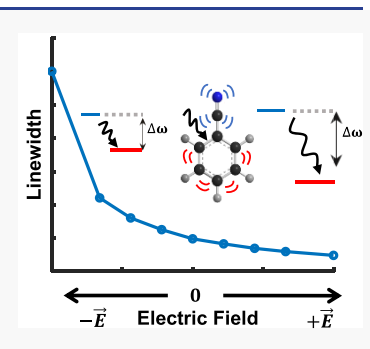
ACCESS

III Metrics & More

Article Recommendations

SI Supporting Information

ABSTRACT: Intramolecular vibrational energy relaxation (IVR) is fundamentally important to chemical dynamics. We show that externally applied electric fields affect IVR and vibrational line widths by changing the anharmonic couplings and frequency detunings between modes. We demonstrate this effect in benzonitrile for which prior experimental results show a decrease in vibrational line width as a function of applied electric field. We identify three major channels for IVR that depend on electric field. In the dominant channel, the electric field affects the frequency detuning, while in the other two channels, variation of anharmonic couplings as a function of field is the underlying mechanism. Consistent with experimental results, we show that the combination of all channels gives rise to reduced line widths with increasing electric field in benzonitrile. Our results are relevant for controlling IVR with external or internal fields and for gaining a more complete interpretation of line widths of vibrational Stark probes.



The importance of electric fields and electrostatic interactions at the molecular length scales in influencing the thermodynamics and kinetics of reactions can not be overstated. The role of electric fields in enzyme catalysis, ^{1,2} electrocatalysis, ^{3,4} and thermocatalysis ^{5,6} is becoming more prominent with new experimental and computational evidence. ⁷ Control over fields at interfaces and microenvironments for enhanced reactivity is a major research frontier. ^{8,9}

A critical tool for measuring electric fields on the molecular scale is vibrational Stark shift spectroscopy. 10-12 A well-defined localized vibration in a probe molecule is first calibrated in electric fields and reference environments. The frequency shift of the reporter molecule is often linearly related to the local electric field. Even though specific interactions of such molecules, such as hydrogen bonding, are more complicated and must be accounted for, they remain valuable reporters of chemical microenvironments such as enzyme cavities 13 and near electrochemical interfaces. 14,15

Benzonitrile is a useful Stark probe because it is relatively unreactive and its nitrile stretch frequency near 2230 cm⁻¹ is isolated from other common vibrations of organic molecules. Frequency shift of nitrile has been used by us and others for understanding a variety of problems ranging from electrostatic fields within proteins, ^{16,17} dielectric solvation and ionic structure near interfaces. ¹⁴

A natural issue in interpretation of nitrile stretch spectra is understanding their line widths. One may envisage at least two sources contributing to the line width. First, the molecule reports on the fluctuations and inhomogeneities of the environment as an antenna, and thereby encodes the environmental variations in its line width. Second, the Stark-active vibration is often coupled to other low frequency modes within the same molecule and can dissipate energy into those modes

thereby contributing to the line width. 19,20 When the second mechanism is operative, interpreting the line widths as merely a representation of the environmental fluctuations via an antenna effect becomes problematic. In this work, we show that not only there is a significant intramolecular source of line broadening in the benzonitrile Stark probe molecule, but also that such intramolecular pathways of energy dissipation change as a function of applied electric field. The second observation is the main point of our work and helps with isolating intra- and intermolecular effects when interpreting Stark shift spectroscopy line widths. In the broader context of intramolecular vibrational energy relaxation, our work emphasizes that such relaxation pathways can be altered by external electric fields, either applied by an electrode or due to a nearby ionic structure. Therefore, these results are applicable when considering reactive pathways that depend on intramolecular vibrational relaxation.

The line width of nitriles has been discussed in the literature previously. It is well-known that not only the nitrile frequency but also the line width is altered by the solvent^{21–24} and temperature.^{21,23} Gai and co-workers on studying nitrile derivatized amino acids have reported red-shift and narrowing in tetrahydrofuran and blue-shift and broadening in water. Temperature-dependent FTIR measurements show narrower line width with increase in temperature and have been attributed to more homogeneous environment at higher temperatures.²¹

Received: July 12, 2021 Accepted: August 5, 2021



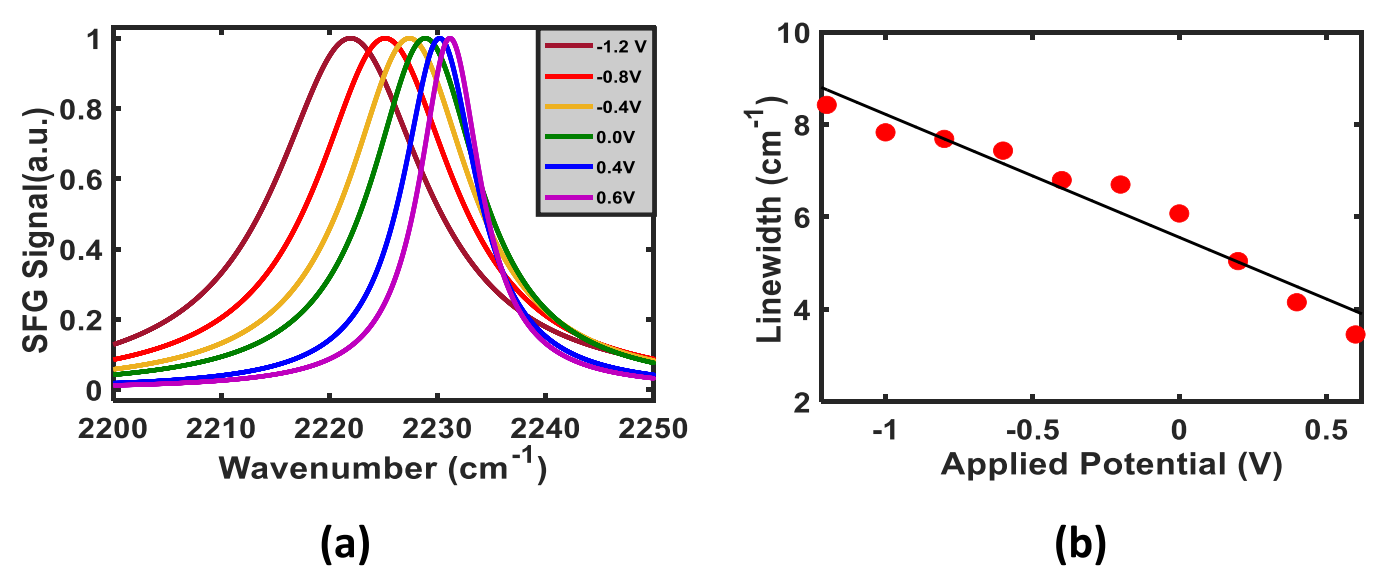


Figure 1. Vibrational sum frequency generation (SFG) spectroscopy data of surface tethered benzonitrile as a function of applied potential. (a) Nitrilestretch spectra and (b) line widths of nitriles. Adapted from reference 44 Copyright 2019 American Chemical Society.

Several decades ago, work on ortho-, meta-, and para-substituted acetophenone by Mueller and co-workers revealed that steric and inductive effects of the substituents play an important role in determining the line widths of the carbonyl.²⁵

Recent experimental and theoretical studies have shown that the nitrile frequency-shift changes the nitrile vibrational lifetime due to intramolecular coupling with other low frequency modes present in the molecule. This is due to alteration of the vibrational energy transfer rate from nitrile to other overtones of the low frequency modes.²⁰ This intramolecular energy dissipation phenomena for the CN mode has been observed in isotopically substituted nitriles. Here, the perturbing factor that changes the intramolecular relaxation is mass. IR pumpprobe measurements of isotopically substituted p-cyanophenylalanine (Phe-CN) by Rodgers et al. revealed a nonmonotonic lifetime trend with respect to reduced mass. 19 As the electronic potential of the molecule does not change due to isotopic substitution, the contributing factor to the nitrile lifetime was due to the intramolecular vibrational relaxation. 20 IR experiments by Tucker et al. showed that by tuning the intramolecular coupling it is possible to tune the vibrational energy flow in p-azidobenzonitrile (PAB) and p-(azidomethyl)benzonitrile (PAMB).²⁶

Outside of the context of Stark shift spectroscopy, long-lived vibrations are important in mediating chemical reactions in gas and condensed phase and in biomolecules. There is interest in vibrational energy and thermal transport through molecules and molecular junctions, $^{30-35}$ including hydrocarbon chains and polyethylene glycol oligomers, in some studies with the aim of designing molecular systems that rectify vibrational energy and thermal transport. The nature and rate of energy and thermal transport in molecular systems are influenced by vibrational energy relaxation.

Recently, we have identified a systematic line width change in the nitrile stretch of benzonitrile with application of an electrochemical potential. He sum frequency generation experiments on tethered 4-mercaptobenzonitrile show line-narrowing with oxidative potentials and line-broadening with reductive potentials (Figure 1, parts a and b). One may suspect that such changes are due to changes in the fluctuations or structure of ions near the electrode. However, no *a priori* reason suggests

that in the mentioned experiment either sign of the electric field should result into reduced or enhanced fluctuations or inhomogeneities.

We have also reported a similar trend as a function of the electron-donation strength of a number of neutral substituents. The more electron donating groups (emulating a negatively biased electrode), in general, cause line-broadening. The above experimental results led us to hypothesize that an intramolecular source of line-broadening, especially one that is sensitive to the externally applied field, is likely the reason for these observations.

In this work we seek to test the hypothesis of electric field-dependent vibrational energy transfer. To our knowledge, intramolecular effects in line broadening from the perspective of a continuously variable external electric field has not been explored before. Two factors govern dissipation of energy from nitrile to lower frequency modes: anharmonic couplings, and resonances between the nitrile and combinations and overtones of lower frequency modes. Correspondingly, we compute how these factors change as the applied electric field on a molecule is varied. Using a standard energy transfer formalism, we show that the combination of these two factors predicts line-narrowing for positive fields and line-broadening for negative fields, consistent with the experimental observations.

To compute the molecular vibrations and anharmonicities in the presence of an electric field, we use a previously reported method.⁴⁵ In brief, two meshes of point charges are created to mimic positive and negative sides of a capacitor. The size of the capacitor and the mesh is selected such that the field is uniform along the body of the molecule. Geometry optimization and frequency calculations were carried out by placing a benzonitrile molecule centered between the two capacitor plates (Figure 2). Density functional theory methods were used for geometry optimization and frequency calculation with the B3LYP functional and the 6-311G(d) basis set using the Q-chem package. 46 IQMol was used as visualization software. All the computations were performed in vacuum. For anharmonic frequencies of benzonitrile, VCI(2) (vibrational configuration interaction theory) was used. We have reported the effect of electric fields ranging from -50 to +50 MV/cm.

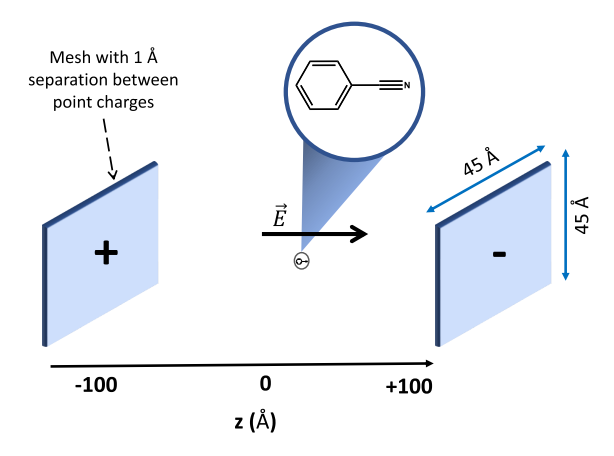


Figure 2. Cartoon of the computational setup used in this study. Adapted with permission from ref 45 Copyright 2018 American Chemical Society.

Third order anharmonic couplings are calculated for geometry optimized structures. These cubic anharmonicities and resonance conditions (or their detuning from CN mode) are crucial in determining the intramolecular effects in the line width of nitrile stretch. To third order in the anharmonic coupling, the rate of energy relaxation from the nitrile, W, is given by the sum of two terms, $W = W_d + W_d$ where⁴⁷

$$W_{d}(\omega_{\alpha}) = \frac{\hbar}{16\omega_{\alpha}} \sum_{\beta,\gamma} \frac{|\Phi_{\alpha\beta\gamma}|^{2} (1 + n_{\beta} + n_{\gamma})}{\omega_{\beta}\omega_{\gamma}}$$

$$\times \frac{(\Gamma_{\alpha} + \Gamma_{\beta} + \Gamma_{\gamma})}{(\omega_{\alpha} - \omega_{\beta} - \omega_{\gamma})^{2} + (\Gamma_{\alpha} + \Gamma_{\beta} + \Gamma_{\gamma})^{2}/4}$$

$$W_{c}(\omega_{\alpha}) = \frac{\hbar}{8\omega_{\alpha}} \sum_{\beta,\gamma} \frac{|\Phi_{\alpha\beta\gamma}|^{2} (n_{\beta} - n_{\gamma})}{\omega_{\beta}\omega_{\gamma}}$$

$$\times \frac{(\Gamma_{\alpha} + \Gamma_{\beta} + \Gamma_{\gamma})}{(\omega_{\alpha} + \omega_{\beta} - \omega_{\gamma})^{2} + (\Gamma_{\alpha} + \Gamma_{\beta} + \Gamma_{\gamma})^{2}/4}$$
(2)

In the above, the subscript α refers to the nitrile vibration, while β and γ refer to the modes that accept energy from nitrile.

The coefficients of the cubic terms in the expansion of the interatomic potential in normal coordinates is $\Phi_{\alpha\beta\gamma}$. The detuning between donor and acceptor modes is $\Delta\omega=\omega_\alpha-\omega_\beta-\omega_\gamma$. The broadening of each mode involved in the transfer is Γ , while the thermal population in the relevant modes is $n=(\exp(\hbar\omega/k_BT)-1)^{-1}$.

Relaxation of the nitrile stretch into two vibrational quanta, either into two different modes or into one mode, is given by eq 1, and is referred to as decay with rate given by W_d . Equation 2 corresponds to the combination of a quantum of the nitrile stretch with a vibrational quantum of a second mode to yield a quantum of vibration in a third mode, with a rate given by W_c . This second process makes negligible contribution to the total rate, W, and thus to the line width of the nitrile. The frequency of the nitrile stretching mode, roughly 2300 cm⁻¹, lies well below the next group of vibrational frequencies, which start above 3000 cm⁻¹. To reach beyond 3000 cm⁻¹ a vibrational quantum of greater than 700 cm⁻¹ is required, and such modes have a low probability to be populated at 300 K. Furthermore, the CH stretch vibrations above 3000 cm⁻¹ tend to be fairly localized and couple only very weakly to the nitrile stretch. We thereby only consider eq 1 in the calculation of the line width, so that W $\approx W_d$. The lifetime contribution to the line width of the nitrile is given by $W\hbar/2$.

The rate of energy relaxation, W, is given by the product of the square of the coupling and the local density of states coupled via cubic anharmonic interactions to the nitrile stretch. The density of states depends on the broadening of all the locally coupled states, represented by Γ_j for mode j. The value of the broadening depends on relaxation rates for all modes due to coupling to other modes and to the solvent. We do not know the solvent contribution, and we have taken the sum of Γ_j in eq 1 to be 24 cm⁻¹ for all the calculations that we report. The rate increases somewhat when we select larger values of this sum, but we are interested here in how the line width varies with the strength of the field, and what gives rise to that variation. Changes in the sum to a different value, e.g., 20 or 50 cm⁻¹, do not affect the trend.

Of course, higher order anharmonic coupling terms may contribute to the rate of relaxation of the nitrile and thus to the line width. In past work, calculation of the nitrile lifetimes of four isotopomers of cyanophenylalanine in solution that incorporated only cubic anharmonic interactions yielded results²⁰ that

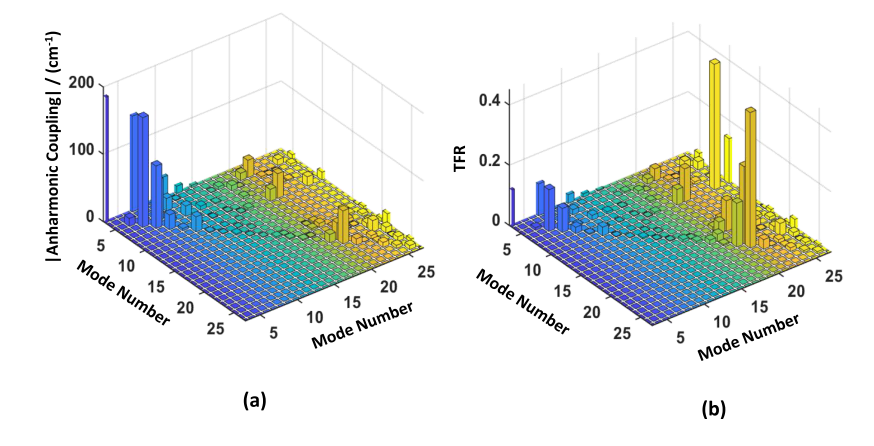


Figure 3. (a) Cubic coupling in the absence of electric field between the CN stretch and combinations of modes β and γ . (b) Third order Fermi resonance (TFR) in the absence of field, which is a scaled version of panel a to account for resonance (eq 3). Since the quantities are symmetric, only half of the coupling and TFR matrices are shown for ease of visualization.

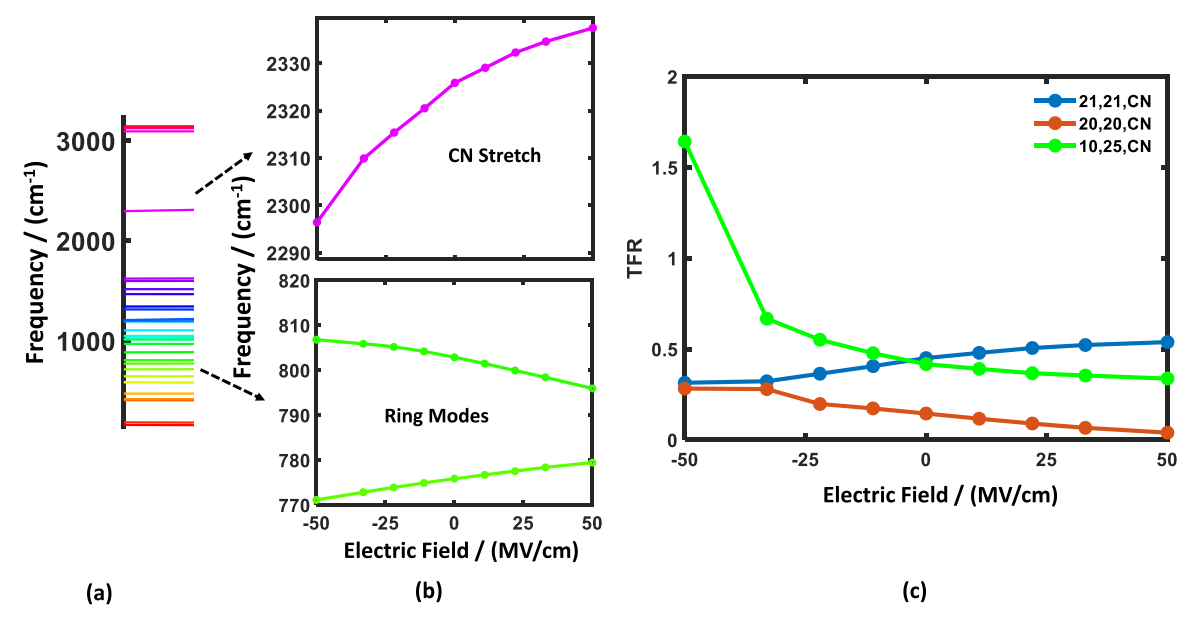


Figure 4. (a) Vibrational manifold of benzonitrile. (b) Variation of several representative modes with electric field. The Stark shift of the CN stretch and the lower frequency modes will affect the resonance condition for energy transfer. (c) Third order Fermi resonance (TFR) for the three important channels of vibrational relaxation as a function of electric field.

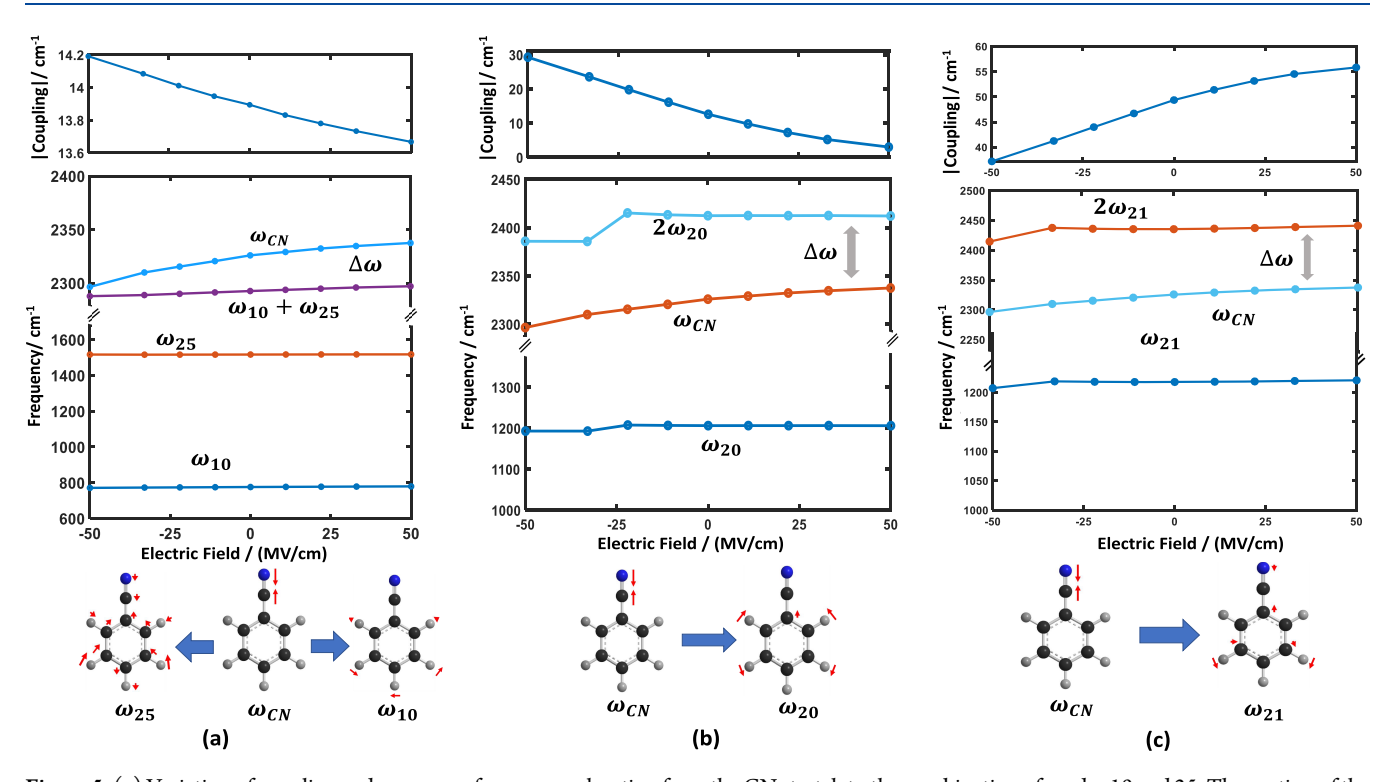


Figure 5. (a) Variation of coupling and resonance for energy relaxation from the CN stretch to the combination of modes 10 and 25. The motion of the atoms in the respective modes are shown below. The detuning increases significantly with more positive fields, giving rise to narrower line widths. (b) Variation of coupling and resonance for energy relaxation from the CN stretch to two quanta of mode 20. The motion of the atoms in the respective modes are shown below. There is an significant decrease in coupling with more positive field, giving rise to narrower line widths. (c) Variation of coupling and resonance for energy relaxation from the CN stretch to two quanta of mode 21. The motion of the atoms in the respective modes are shown below. The coupling increases significantly with more positive field.

compared well with experimental measurements carried out by Gai and co-workers. ¹⁹ Not only did the rates of energy relaxation compare well but also trends in the rates with isotopic substitution reproduced the trends found in the experiments. In general, we expect that the anharmonic contribution to rates of energy relaxation in molecules of moderate size, or larger as

considered in this study and in the earlier study of cyanophenylalanine, is on average dominated by cubic terms. We carried out calculations of the rate of energy transfer from the nitrile, and thereby the line width, using the mode frequencies and cubic anharmonic coupling at nine different field strengths.

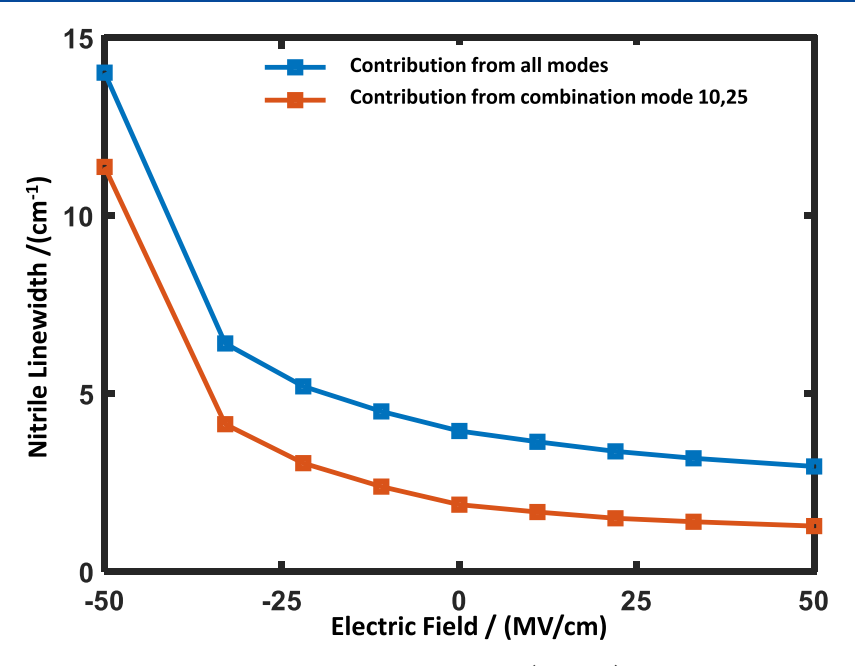


Figure 6. Computed nitrile line widths as a function of electric field due to all channels (blue line) and the dominant channel (orange). Consistent with experimental results, the line width narrows with a more positive field.

As shown in eq 1, two factors determine energy transfer from nitrile to lower frequency modes: anharmonic couplings and resonance between the coupled modes. We will begin by discussing the third order anharmonic couplings between the nitrile vibration (mode 28) and lower frequency modes (modes 3 to 27) without an external field. Figure 3a shows the magnitude of coupling $|\Phi_{CN,\beta,\gamma}|$ as a function of mode number β and γ . The two lowest frequency modes are not included because coupling to them could not be calculated by the electronic structure method used by us. This is not significantly prohibitive since these modes are largely off resonant.

The couplings shown in Figure 3a alone are not enough to determine energy transfer rates. The resonance condition $\Delta\omega=\omega_{\rm CN}-\omega_{\beta}-\omega_{\gamma}$ must also be considered. For that reason, we evaluated an effective dimensionless third order Fermi resonance (TFR) parameter²⁰ that accounts for both coupling and resonance as defined below:

$$TFR = \frac{|\Phi_{\text{CN},\beta,\gamma}|}{\Delta\omega} \tag{3}$$

Figure 3b shows a plot of this parameter, and exhibits a few combinations that dominate energy transfer to low frequency modes. The first of these combinations involves energy transfer from nitrile to one quantum of mode 10 and one quantum of mode 25 ($\omega_{10} = 776 \text{ cm}^{-1}$ and $\omega_{25} = 1517 \text{ cm}^{-1}$). The second dominant contribution is energy transfer to two quanta of mode 21 ($\omega_{21} = 1218 \text{ cm}^{-1}$). Beyond that, there are a few other modes with similar TFR, however, some of them did not show significant variation with electric field. One channel with moderate TFR involves energy transfer to two quanta of mode 20 ($\omega_{20} = 1206 \text{ cm}^{-1}$), which as we will show later does have dependence on electric field.

When the electric field is turned on, the couplings and resonances discussed above are expected to change. Several of the low frequency modes exhibit Stark shifts as a function of field, which can affect their resonance with the nitrile. To exhibit this point, some of the Stark shifting modes are presented in parts a and b of Figure 4. The couplings are also expected to vary.

To understand the combined effect of coupling and resonance in the presence of electric field, we have analyzed the TFRs for the above-mentioned three dominant channels (Figure 4c), and we have noticed that these channels remain dominant for all fields. However, their contributions to energy transfer varies as the electric field is changed either due to change in resonance or the coupling.

For the first channel (mode 10, 25) the coupling does not change significantly as a function of electric field (Figure 5a). However, the resonance condition $\Delta\omega$ varies significantly from the negative electric field (8.6 cm⁻¹ at -50 MV/cm) to positive field (40.4 cm⁻¹ at +50 MV/cm). As this channel becomes more off-resonant with increasing field values, energy transfer becomes less favorable, and consequently its contribution to line width decreases. This is consistent with experimental observation as will be discussed in detail shortly.

For the second channel (mode 20) there is no considerable change in resonance condition as a function of field (Figure 5b). However, the coupling decreases significantly from the negative field (29.3 cm $^{-1}$ at -50 MV/cm) to positive field (3.0 cm $^{-1}$ at +50 MV/cm). This observation is also consistent with decreased line width with increasing field.

In contrast to the second channel, for the third channel (mode 21) the resonance condition does not change much as a function of field (Figure 5c). However, there is an appreciable increase in coupling from the negative field (37.2 cm $^{-1}$ at -50 MV/cm) to positive field (55.8 cm $^{-1}$ at +50 MV/cm). This third channel if evaluated separately would result in larger line widths with increasing field, which is inconsistent with the experimental observations. However, its contribution is largely overwhelmed by the other two channels described above.

To identify the contributions of all combinations, including the above three channels, to the line width we evaluated eq 1. Our results are presented in Figure 6. The figure shows that the line width decreases monotonically from negative to positive fields, consistent with experimental observations. The figure also shows that the contribution of the first channel (coupling to modes 10 and 25) by far is the largest and dominates the trend.

The contribution to the line width from the second and third dominant channels (mode 20, mode 21) are far smaller and not shown.

Note that the span of electric fields studied computationally is larger than the experimentally achievable range. The controllable parameter in the experimental results shown in Figure 1 is the applied potential, which ranges from -1.2 to +0.6 V with respect to Ag/AgCl. As explained in detail in the literature, ⁴⁴ this range corresponds to effective field values spanning \sim 25 MV/cm. Therefore, within the range of fields that are achieved in the experiments, the computational results (Figure 6) show a nearly linear decrease in line width consistent with the experimental observations (Figure 1b). We note that the computed line width at zero electric field is comparable to the line width at zero applied potential (Figure 1) and the previously reported homogeneous line width for benzonitrile derivatives as determined by 2D IR spectroscopy. ⁴⁸

Given that the choice of the solvent contribution to line widths in eq 1 (Γ_{α} , Γ_{β} and Γ_{γ}) can influence the total predicted line width, we do not anticipate quantitatively matching the line widths between computation and experiments. Our goal is to demonstrate that the experimental trend in line widths is reproduced computationally.

For channel 2 and channel 3, the anharmonic coupling is largely varying with electric fields and they show opposite trends. To explain how the electric field influences the coupling between the CN stretch and the modes in these channels, we propose that the motion of the shared carbon atom (C1, shown in Figure 7)

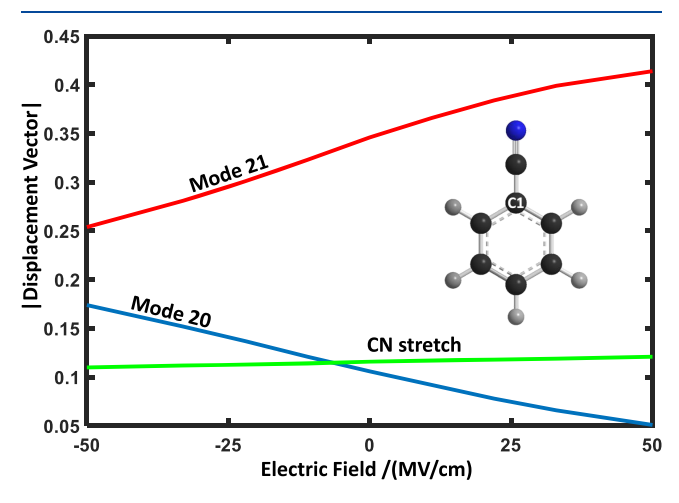


Figure 7. Relative amplitude of the displacement of the shared carbon atom C_1 as a function of electric field.

must be influenced by the electric field. This atom serves as a bridge connecting nitrile to benzene ring. As seen in Figure 7, the amplitude of the C1 atom in the nitrile stretch is small, but remains nearly constant across all fields. However, the amplitude of C1 atom in mode 20 decreases, while in mode 21, it increases with positive field. This justifies the change in coupling shown in Figure 5, parts b and c.

In conclusion, our major finding is demonstrating that IVR and line width can depend on the local electric field felt by the molecule. The electric field affects IVR via changing the anharmonic couplings and/or the resonances between high and low frequency modes. This finding is important for interpreting the vibrational line width of molecules that are used as Stark shift probes. It may be convenient to assign changes in line width of such molecules to fluctuations and

variations of electric field in their environments, as has been reported. 21-24 Here we point out that intramolecular sources of line broadening, and more importantly, their electric-field dependence should not be ignored. Of course, the trend of decreasing line width with increasing field is a consequence of the resonances and couplings for this particular molecule. It should not be generalized to systems that are very different from benzonitrile. For other molecules, such effects may be present; however, they need to be studied separately.

Our work is also relevant to the area of controlling vibrational energy relaxation, and other phenomena that are influenced by vibrational resonances. Note that the source of electric field that influences molecular phenomena need not arise from an electrode. Molecular scale electric fields can also be controllably exerted by the choice of nearby ions 14,49 and solvents. The influence of field on tuning vibrations must be evaluated to understand a broad range of chemical phenomena. A few examples include the role of bridging groups in transferring vibrational energy, 50,51 electrons, 52 and protons. 51 In such cases, one may use electric fields to tune the frequency and couplings of vibrations that control these processes.

ASSOCIATED CONTENT

Supporting Information

The Supporting Information is available free of charge at https://pubs.acs.org/doi/10.1021/acs.jpclett.1c02238.

Input geometry of benzonitrile, computed frequencies of all vibrational modes, and the third order anharmonic couplings between CN and other modes (PDF)

AUTHOR INFORMATION

Corresponding Author

Jahan M. Dawlaty — Department of Chemistry, University of Southern California, Los Angeles, California 90089-0001, United States; ⊚ orcid.org/0000-0001-5218-847X; Email: dawlaty@usc.edu

Authors

Anwesha Maitra – Department of Chemistry, University of Southern California, Los Angeles, California 90089-0001, United States

Sohini Sarkar – Department of Chemistry, University of Southern California, Los Angeles, California 90089-0001, United States; oorcid.org/0000-0002-5714-6778

David M. Leitner — Department of Chemistry, University of Nevada Reno, Reno, Nevada 89519, United States;
orcid.org/0000-0002-3105-818X

Complete contact information is available at: https://pubs.acs.org/10.1021/acs.jpclett.1c02238

Notes

The authors declare no competing financial interest.

ACKNOWLEDGMENTS

This work was supported by the Air Force Office of Scientific Research under AFOSR Award FA9550-18-1-0420. A.M. was partially supported by the Research Corporation for Science Advancement (RCSA) Scialog Award 27145. S.S. was partially supported by the Research Corporation for Science Advancement (RCSA) through their Cottrell Fellowship for ensuring continuity of funding for postdoctoral scholars under Award 27445 and cosponsored by the National Science Foundation

under Award CHE-2039044. D.M.L. was supported by NSF CHE-1854271.

REFERENCES

- (1) Warshel, A.; Sharma, P. K.; Kato, M.; Xiang, Y.; Liu, H.; Olsson, M. H. M. Electrostatic Basis for Enzyme Catalysis. *Chem. Rev.* **2006**, *106*, 3210–3235.
- (2) Fried, S. D.; Boxer, S. G. Electric Fields and Enzyme Catalysis. *Annu. Rev. Biochem.* **2017**, *86*, 387–415.
- (3) Rhodes, C. J. Electric Fields in Zeolites: Fundamental Features and Environmental Implications‡. *Chem. Pap.* **2016**, *70*, 4–21.
- (4) Che, F.; Gray, J. T.; Ha, S.; Kruse, N.; Scott, S. L.; McEwen, J.-S. Elucidating the Roles of Electric Fields in Catalysis: A Perspective. *ACS Catal.* **2018**, *8*, 5153–5174.
- (5) Das, S.; Pérez-Ramírez, J.; Gong, J.; Dewangan, N.; Hidajat, K.; Gates, B. C.; Kawi, S. Core—shell Structured Catalysts for Thermocatalytic, Photocatalytic, and Electrocatalytic Conversion of CO2. *Chem. Soc. Rev.* **2020**, *49*, 2937–3004.
- (6) Wesley, T. S.; Román-Leshkov, Y.; Surendranath, Y. Spontaneous Electric Fields Play a Key Role in Thermochemical Catalysis at MetalLiquid Interfaces. *ACS Cent. Sci.* **2021**, *7*, 1045–1055.
- (7) Suydam, I. T.; Snow, C. D.; Pande, V. S.; Boxer, S. G. Electric Fields at the Active Site of an Enzyme: Direct Comparison of Experiment with Theory. *Science* **2006**, *313*, 200–204.
- (8) Bím, D.; Alexandrova, A. N. Local Electric Fields As a Natural Switch of Heme-Iron Protein Reactivity. *ACS Catal.* **2021**, *11*, 6534–6546.
- (9) Shaik, S.; Mandal, D.; Ramanan, R. Oriented Electric Fields as Future Smart Reagents in Chemistry. *Nat. Chem.* **2016**, *8*, 1091–1098.
- (10) Walker, D. M.; Hayes, E. C.; Webb, L. J. Vibrational Stark Effect Spectroscopy reveals Complementary Electrostatic Fields created by Protein—protein Binding at the Interface of Ras and Ral. *Phys. Chem. Chem. Phys.* **2013**, *15*, 12241—12252.
- (11) Park, E. S.; Andrews, S. S.; Hu, R. B.; Boxer, S. G. Vibrational Stark Spectroscopy in Proteins: A Probe and Calibration for Electrostatic Fields. *J. Phys. Chem. B* **1999**, *103*, 9813–9817.
- (12) Slocum, J. D.; Webb, L. J. Measuring Electric Fields in Biological Matter Using the Vibrational Stark Effect of Nitrile Probes. *Annu. Rev. Phys. Chem.* **2018**, *69*, 253–271.
- (13) Fafarman, A. T.; Webb, L. J.; Chuang, J. I.; Boxer, S. G. Site-Specific Conversion of Cysteine Thiols into Thiocyanate Creates an IR Probe for Electric Fields in Proteins. *J. Am. Chem. Soc.* **2006**, *128*, 13356–13357.
- (14) Sarkar, S.; Maitra, A.; Banerjee, S.; Thoi, V. S.; Dawlaty, J. M. Electric Fields at Metal—Surfactant Interfaces: A Combined Vibrational Spectroscopy and Capacitance Study. *J. Phys. Chem. B* **2020**, *124*, 1311—1321.
- (15) Patrow, J. G.; Sorenson, S. A.; Dawlaty, J. M. Direct Spectroscopic Measurement of Interfacial Electric Fields near an Electrode under Polarizing or Current-Carrying Conditions. *J. Phys. Chem. C* 2017, 121, 11585–11592.
- (16) Deb, P.; Haldar, T.; Kashid, S. M.; Banerjee, S.; Chakrabarty, S.; Bagchi, S. Correlating Nitrile IR Frequencies to Local Electrostatics Quantifies Noncovalent Interactions of Peptides and Proteins. *J. Phys. Chem. B* **2016**, *120*, 4034–4046.
- (17) Jo, H.; Culik, R. M.; Korendovych, I. V.; DeGrado, W. F.; Gai, F. Selective Incorporation of Nitrile-Based Infrared Probes into Proteins via Cysteine Alkylation. *Biochemistry* **2010**, *49*, 10354–10356.
- (18) Sorenson, S. A.; Patrow, J. G.; Dawlaty, J. M. Solvation Reaction Field at the Interface Measured by Vibrational Sum Frequency Generation Spectroscopy. *J. Am. Chem. Soc.* **2017**, *139*, 2369–2378.
- (19) Rodgers, J. M.; Zhang, W.; Bazewicz, C. G.; Chen, J.; Brewer, S. H.; Gai, F. Kinetic Isotope Effect Provides Insight into the Vibrational Relaxation Mechanism of Aromatic Molecules: Application to Cyanophenylalanine. *J. Phys. Chem. Lett.* **2016**, *7*, 1281–1287.
- (20) Pandey, H. D.; Leitner, D. M. Vibrational States and Nitrile Lifetimes of Cyanophenylalanine Isotopomers in Solution. *J. Phys. Chem. A* **2018**, *122*, 6856–6863.

- (21) Getahun, Z.; Huang, C.-Y.; Wang, T.; De León, B.; DeGrado, W. F.; Gai, F. Using Nitrile-Derivatized Amino Acids as Infrared Probes of Local Environment. *J. Am. Chem. Soc.* **2003**, *125*, 405–411.
- (22) Lindquist, B. A.; Corcelli, S. A. Nitrile Groups as Vibrational Probes: Calculations of the CN Infrared Absorption Line Shape of Acetonitrile in Water and Tetrahydrofuran. *J. Phys. Chem. B* **2008**, *112*, 6301–6303
- (23) Maienschein-Cline, M. G.; Londergan, C. H. The CN Stretching Band of Aliphatic Thiocyanate is Sensitive to Solvent Dynamics and Specific Solvation. *J. Phys. Chem. A* **2007**, *111*, 10020–10025.
- (24) Mojica, E.-R. E.; Abbas, N.; Wyan, L. O.; Vedad, J.; Desamero, R. Z. B. Solvent Sensitivity of the −C≡N Group: A Raman Spectroscopic Study. *ACS Symp. Ser.* **2018**, *1305*, 181−197.
- (25) Jones, Ř. Ñ.; Forbes, W. F.; Mueller, W. A. The Infrared Carbonyl Stretching band of Ring substituted Acetophenones. *Can. J. Chem.* **1957**, 35, 504–514.
- (26) Schmitz, A. J.; Pandey, H. D.; Chalyavi, F.; Shi, T.; Fenlon, E. E.; Brewer, S. H.; Leitner, D. M.; Tucker, M. J. Tuning Molecular Vibrational Energy Flow within an Aromatic Scaffold via Anharmonic Coupling. *J. Phys. Chem. A* **2019**, *123*, 10571–10581.
- (27) Leitner, D. M. Influence of Quantum Energy flow and Localization on Molecular Isomerization in Gas and Condensed Phases. *Int. J. Quantum Chem.* **1999**, *75*, 523–531.
- (28) Leitner, D. M. Quantum Ergodicity and Energy flow in Molecules. *Adv. Phys.* **2015**, *64*, 445–517.
- (29) Yadav, P. K.; Keshavamurthy, S. Breaking of a Bond: When is it Statistical? *Faraday Discuss.* **2015**, 177, 21–32.
- (30) Rubtsova, N. I.; Rubtsov, I. V. Vibrational Energy Transport in Molecules studied by Relaxation-assisted Two-dimensional Infrared Spectroscopy. *Annu. Rev. Phys. Chem.* **2015**, *66*, 717–738.
- (31) Yue, Y.; Qasim, L. N.; Kurnosov, A. A.; Rubtsova, N. I.; Mackin, R. T.; Zhang, H.; Zhang, B.; Zhou, X.; Jayawickramarajah, J.; Burin, A. L.; Rubtsov, I. V. Band-selective Ballistic energy Transport in Alkane Oligomers: Toward Controlling the Transport Speed. *J. Phys. Chem. B* **2015**, *119*, 6448–6456.
- (32) Rubtsov, I. V.; Burin, A. L. Ballistic and Diffusive Vibrational Energy Transport in Molecules. *J. Chem. Phys.* **2019**, *150*, 020901.
- (33) Segal, D.; Agarwalla, B. K. Vibrational Heat Transport in Molecular Junctions. *Annu. Rev. Phys. Chem.* **2016**, *67*, 185–209.
- (34) Kalantar, N. K.; Agarwalla, B. K.; Segal, D. On the Definitions and Simulations of Vibrational Heat Transport in Nanojunctions. *J. Chem. Phys.* **2020**, *153*, 174101.
- (35) Dinpajooh, M.; Nitzan, A. Heat Conduction in Polymer Chains with Controlled End-to-end Distance. *J. Chem. Phys.* **2020**, *153*, 164903.
- (36) Leong, T. X.; Qasim, L. N.; Mackin, R. T.; Du, Y.; Pascal, R. A.; Rubtsov, I. V. Unidirectional Coherent Energy Transport via Conjugated Oligo(p -phenylene) Chains. *J. Chem. Phys.* **2021**, *154*, 134304.
- (37) Pein, B. C.; Sun, Y.; Dlott, D. D. Controlling Vibrational Energy flow in Liquid Alkylbenzenes. *J. Phys. Chem. B* **2013**, *117*, 10898–10904.
- (38) Pein, B. C.; Sun, Y.; Dlott, D. D. Unidirectional Vibrational Energy flow in Nitrobenzene. *J. Phys. Chem. A* **2013**, *117*, 6066–6072. (39) Pein, B. C.; Dlott, D. D. Modifying Vibrational Energy flow in
- Aromatic Molecules: Effects of Ortho Substitution. *J. Phys. Chem. A* **2014**, *118*, 965–973.
- (40) Leitner, D. M.; Pandey, H. D. Asymmetric Energy flow in Liquid Alkylbenzenes: A Computational Study. *J. Chem. Phys.* **2015**, *143*, 144301.
- (41) Segal, D.; Nitzan, A. Heat Rectification in Molecular Junctions. *J. Chem. Phys.* **2005**, 122, 194704.
- (42) Leitner, D. M. Thermal Boundary Conductance and Thermal Rectification in Molecules. *J. Phys. Chem. B* **2013**, *117*, 12820–12828. (43) Reid, K. M.; Pandey, H. D.; Leitner, D. M. Elastic and Inelastic Contributions to Thermal Transport between Chemical Groups and

Thermal Rectification in Molecules. J. Phys. Chem. C 2019, 123, 6256-

6264.

- (44) Sarkar, S.; Patrow, J. G.; Voegtle, M. J.; Pennathur, A. K.; Dawlaty, J. M. Electrodes as Polarizing Functional Groups: Correlation between Hammett Parameters and Electrochemical Polarization. *J. Phys. Chem. C* **2019**, *123*, 4926–4937.
- (45) Patrow, J. G.; Wang, Y.; Dawlaty, J. M. Interfacial Lewis Acid—Base Adduct Formation Probed by Vibrational Spectroscopy. *J. Phys. Chem. Lett.* **2018**, *9*, 3631–3638.
- (46) Shao, Y.; et al. Advances in Molecular Quantum Chemistry Contained in the Q-Chem. 4 Program Package. *Mol. Phys.* **2015**, *113*, 184–215.
- (47) Fabian, J.; Allen, P. B. Anharmonic Decay of Vibrational States in Amorphous Silicon. *Phys. Rev. Lett.* **1996**, *77*, 3839–3842.
- (48) Ma, J.; Pazos, I. M.; Gai, F. Microscopic Insights into the Protein-stabilizing Effect of Trimethylamine N-oxide (TMAO). *Proc. Natl. Acad. Sci. U. S. A.* **2014**, *111*, 8476–8481.
- (49) Thammavongsy, Z.; Cunningham, D. W.; Sutthirat, N.; Eisenhart, R. J.; Ziller, J. W.; Yang, J. Y. Adaptable Ligand Donor Strength: Tracking Transannular Bond Interactions in Tris(2-pyridylmethyl)-azaphosphatrane (TPAP). *Dalton Trans* **2018**, 47, 14101–14110.
- (50) Rafiq, S.; Bezdek, M. J.; Chirik, P. J.; Scholes, G. D. Dinitrogen Coupling to a Terpyridine-Molybdenum Chromophore Is Switched on by Fermi Resonance. *Chem.* **2019**, *5*, 402–416.
- (51) Lin, Z.; Lawrence, C. M.; Xiao, D.; Kireev, V. V.; Skourtis, S. S.; Sessler, J. L.; Beratan, D. N.; Rubtsov, I. V. Modulating Unimolecular Charge Transfer by Exciting Bridge Vibrations. *J. Am. Chem. Soc.* **2009**, 131, 18060–18062.
- (52) Delor, M.; Scattergood, P. A.; Sazanovich, I. V.; Parker, A. W.; Greetham, G. M.; Meijer, A. J. H. M.; Towrie, M.; Weinstein, J. A. Toward Control of Electron Transfer in Donor-acceptor Molecules by Bond-specific Infrared Excitation. *Science* **2014**, *346*, 1492–1495.